

Hardware Impairments-Aware Transceiver Design for Multi-Carrier Full-Duplex MIMO Relaying

Vimal Radhakrishnan, *Member, IEEE*, Omid Taghizadeh, *Member, IEEE*, Rudolf Mathar, *Senior Member, IEEE*

Abstract—In this work, we study the linear precoding and decoding design problem for a full-duplex (FD) multi-carrier (MC) decode and forward (DF) relaying system, under multiple sources of impairments. In particular, the impact of non-linear hardware distortions at the transmit and receiver chains, leading to residual self-interference (SI) and inter-carrier leakage (ICL), as well as the imperfect channel state information (CSI) are taken into account. In the first step, the known time-domain characterization of hardware impairments is transformed over a general orthonormal MC basis. As a result, the problem of linear precoding and decoding design is formulated to maximize the MC system sum-rate, however, leading to a non-convex mathematical structure. An alternating quadratic convex program (AQCP) is consequently proposed, with a monotonic improvement at each iteration, leading to a guaranteed convergence. The proposed AQCP framework is then extended, employing the Dinkelbach algorithm, in order to maximize the system energy efficiency in terms of bits-per-Joule. The proposed design strategies are considered both for per-subcarrier as well as the joint-subcarrier coding strategies, wherein the latter case the coding is performed jointly over all subcarriers. Numerical simulations show a significant gain in the performance of the proposed algorithms compared to the half-duplex (HD) counterparts or to the solutions where the impact of impairments are not considered, particularly when the hardware accuracy is not very high.

I. INTRODUCTION

The fifth generation mobile communication networks (5G) has established the goal of extending the service domain of the traditional wireless networks for an ever increasing number of users, by introducing diverse use cases and service specifications [2]. In particular, with almost all of the sub 6 GHz spectrum already assigned, the expected rapid increase in the wireless data traffic calls for spectrally-efficient access solutions, while extending the coverage of the available infrastructure to a wider region and number of users. In the conventional communication systems, the nodes either transmit or receive at the same time-frequency channel resource. In

contrast, full-duplex (FD) nodes are allowed to transmit and receive simultaneously over the same frequency, thereby showing potential to enhance the spectral efficiency [3]. However, they inherently suffer from the strong self-interference (SI) from their own transmitter. Recently, efficient self-interference cancellation (SIC) techniques are developed [4]–[9], which made it feasible to incorporate FD transceivers into the future communication systems¹ [10], [11] and motivated several related studies on the promising use-cases, e.g., in-band bidirectional communication [12]–[15], FD-enabled jamming for improving physical layer [16], [17], self-backhauling [18] and FD cellular networking [19]–[21].

As a promising use-case, FD-relays have been the focus of several recent studies due to their potential to improve network coverage, spectral efficiency and to reduce latency, thanks to concurrent transmission and reception at the same channel. In particular, it is shown in [22]–[24] that FD relays with decode and forward (DF) processing are more robust against the impact of hardware impairments against their amplify-and-forward (AF) counterpart, due to the distortion-amplification effect observed in FD-AF relays. The problems regarding optimal resource allocation and performance analysis for the single carrier FD DF relaying systems have been the focus of recent works [9], [13], [25]–[31]. In [25], a convergent block coordinate ascent algorithm is proposed for the maximization of end-to-end achievable rate by taking into account the practical factor of limited dynamic range. In [26] an FD DF relaying system is studied with the consideration of erroneous channel state information (CSI) and limited SIC following a worst-case performance guarantee approach, and later extended to a multi-user scenario [27]. Consideration of simultaneous wireless information and power transfer (SWIPT) for a FD DF relay network is investigated in [28]. The outage performance of FD DF relaying with the limited dynamic range has been the focus of [29], [30].

For the FD DF systems operating with a multi-carrier (MC) protocol, the problems regarding MC resource allocation and system performance analysis have been studied in [32]–[36]. Please note that this scenario serves well for extending the network coverage for a large number of users due to the multi-carrier FD relaying capability, as an instance of coverage extension for a massive machine-type communication (mMTC)

Copyright (c) 2015 IEEE. Personal use of this material is permitted. However, permission to use this material for any other purposes must be obtained from the IEEE by sending a request to pubs-permissions@ieee.org.

V. Radhakrishnan and R. Mathar are with the Institute for Theoretical Information Technology, RWTH Aachen University, Aachen, 52074, Germany (email: {radhakrishnan, mathar}@ti.rwth-aachen.de).

O. Taghizadeh is with the Network Information Theory Group, Technische Universität Berlin, 10587 Berlin, Germany (email: {taghizadehmotlagh}@tu-berlin.de). This work has been supported by Deutsche Forschungsgemeinschaft (DFG), under the Grant No. MA 1184/38 – 1.

Part of this work has been presented in WSA 2018, 22nd International ITG Workshop on Smart Antennas [1].

¹Please note that the FD systems requires more complex implementations for SIC in terms of additional hardware as well as signal processing. Combinations of SIC techniques, for example, cross-polarization [4], antenna cancellation techniques [5], RF circulators [8], SI suppression schemes [9], to name a few, are needed to be implemented together to effectively cancel out the SI in both analog (also to avoid saturation of receiver chain components) and digital domain.

scenario [37], as well as to provide more efficient solutions for an enhanced mobile broadband (eMBB) by improving the spectral and energy efficient connection, thanks to the FD capability of the relay node [38]. In [32], the authors consider an FD multiple-input multiple-output (MIMO) orthogonal frequency division multiplexing (OFDM) DF relay network and derive efficient solutions for source and relay precoding. In [33], a power allocation strategy is presented for a single antenna DF relaying system with the consideration of the direct source-destination link. The end-to-end performance, in terms of outage probability has been derived for multi-hop FD DF OFDM systems in [34], and with the consideration of linear parameter errors in [36].

The aforementioned literature introduce resource allocation strategies for multi-carrier FD DF relaying systems under a perfect/linear hardware assumption, or considering a single carrier or single antenna relay setup. Please note that the consideration of non-linear hardware impairments is particularly important for MC FD transceivers, as it leads to residual SI and inter-carrier leakage² (ICL) and thereby necessitates an impairments-aware design of the transceiver strategy.

A. Contribution

In this paper, we study an FD MC MIMO DF relaying system, from the aspects of spectral and energy efficient resource allocation and performance analysis, where the effect of non-linear hardware distortions, leading to residual SI and ICL, as well as the impact of CSI error are jointly taken into account. The main contributions of this paper are as follows:

- In the first step, we transform the available time-domain characterization of the hardware distortions for an FD transceiver [12], [13], [39] for a general MC system with orthonormal waveforms, e.g., orthogonal variable spreading factor (OVSF) - code division multiple access (CDMA) and the variations of orthogonal frequency division multiple access (OFDMA). Consequently, the end-to-end achievable rate is formulated, employing the obtained characterization. Please note that this is in contrast to the prior works considering the impact of hardware impairments for a single-carrier system [9], [13], [25]–[30], or for a MC relaying system with an accurate/linear hardware [32], [34], [36] or a single antenna setup [33].
- Building on the obtained characterization, in Section III-C, we formulate the linear transceiver design problem for maximizing the system sum-rate, leading to a non-convex problem. An alternating quadratic convex program (AQCP) is then proposed with a monotonic improvement towards convergence. The proposed design is utilized both for per-subcarrier as well as the joint-subcarrier coding strategies, where in the latter case the coding/de-coding is performed jointly over all subcarriers.

²Unlike the purely linear systems, a transmission at any subcarrier leads to an amplified level of impairments at all subcarriers, due to the non-linear nature of impairments.

- The proposed AQCP design framework is then extended, employing the Dinkelbach algorithm, where a double-loop algorithm is proposed in order to maximize the system energy efficiency in terms of bits-per-Jouhl.

Numerical simulations show a significant gain by utilizing distortion-aware design, particularly when the hardware accuracy degrades and hence the residual SI and ICL become a dominant factor.

B. Mathematical Notation

Throughout this paper, we denote the vectors and matrices by lower-case and upper-case bold letters, respectively. We use $\mathbb{E}\{\cdot\}$, $|\cdot|$, $\text{Tr}(\cdot)$, $(\cdot)^{-1}$, $(\cdot)^*$, $(\cdot)^T$, and $(\cdot)^H$ for mathematical expectation, determinant, trace, inverse, conjugate, transpose, and Hermitian transpose, respectively. We use $\text{diag}(\cdot)$ for the diag operator, which returns a diagonal matrix by setting off-diagonal elements to zero. We denote an all zero matrix of size $m \times n$ by $\mathbf{0}_{m \times n}$. We represent the Euclidean norm as $\|\cdot\|_2$. We denote the set of real, positive real, and complex numbers as \mathbb{R} , \mathbb{R}^+ , and \mathbb{C} respectively.

II. SYSTEM MODEL

We consider an FD MC MIMO DF relay which connects a half-duplex (HD) MC MIMO source node equipped with N_s transmit antenna to an HD MC MIMO destination node equipped with M_d receive antennas. The number of transmit and receive antennas at the relay can be denoted as N_r and M_r , respectively. Initially, the source transmits the signal to the relay through the channel $\mathbf{H}_{\text{sr}}^k \in \mathbb{C}^{M_r \times N_s}$ with sub-carrier $k \in \mathbb{K}$, where $\mathbb{K} := \{1, 2, \dots, K\}$ and K is the total number of sub-carriers. At the relay, after applying SIC, the received signal is decoded. Then, the relay transmits the decoded signal to the destination through the channel $\mathbf{H}_{\text{rd}}^k \in \mathbb{C}^{M_d \times N_r}$. Due to SI at the relay, a part of the transmitted signal is received by the relay itself through the SI channel $\mathbf{H}_{\text{rr}}^k \in \mathbb{C}^{M_r \times N_r}$. Similar to [13], [40], we also consider a weak signal (due to path loss) from the source is received at the destination through the direct channel $\mathbf{H}_{\text{sd}}^k \in \mathbb{C}^{M_d \times N_s}$, which is considered as interference. We assume all channels are constant for each frame, frequency flat in each sub-carrier and only the imperfect CSI is known.

A. Imperfect Channel State Information

We adapt the channel error model used in [13], [39], where the true channel can be decomposed into the estimated channel plus estimation error, which can be stated as

$$\mathbf{H}_{\mathcal{X}} = \hat{\mathbf{H}}_{\mathcal{X}} + \tilde{\mathbf{H}}_{\mathcal{X}}, \quad \tilde{\mathbf{H}}_{\mathcal{X}} = \mathbf{D}_{\mathcal{X}}^{\frac{1}{2}} \boldsymbol{\Delta}_{\mathcal{X}}, \quad (1)$$

where $\mathcal{X} \in \{\text{sr}, \text{rd}, \text{rr}, \text{sd}\}$, $\hat{\mathbf{H}}_{\mathcal{X}}$ represents the estimated channel, and the entries of $\boldsymbol{\Delta}_{\mathcal{X}}$ are independent and identically distributed (i.i.d.) complex Gaussian with zero mean and a variance of one³. $\mathbf{D}_{\mathcal{X}}$ shapes the spatial covariance matrix of the CSI estimation error. However, we consider that the

³In this work, we consider a synchronized relay channel where time synchronization for each link is implemented at the receiver. Nevertheless, the impact of imperfect time-synchronization appears as a channel phase rotation, which is considered as a part of the CSI error model.

receiver performs a minimum mean square error (MMSE) channel estimation. We also assume the estimated channel and estimation error becomes uncorrelated [24], i.e., $\hat{\mathbf{H}}_{\mathcal{X}} \perp \tilde{\mathbf{H}}_{\mathcal{X}}$.

B. CSI estimation protocol

Similar to [13], [39], we consider the coherence time interval T_{tot} is partitioned into training and data communication period; i.e., there exists a training period T_{train} before the data communication period. The training period is further partitioned into two equal-length periods (i.e., $T_{\text{train}}[1]$ and $T_{\text{train}}[2]$) to avoid self-interference when estimating the channel matrices. During $T_{\text{train}}[1]$, the relay and destination estimates the CSI of their respective channel from the source. Subsequently, during $T_{\text{train}}[2]$, the destination estimates the channel from the relay, where as the relay estimates its self-interference channel. Using the estimated CSI, the design parameters are optimized and utilized for the data communication. Furthermore, in order to overcome the issue of a attacks in wireless OFDM while utilizing the convectional channel training protocol using pilot tones, a secure and stable channel training authentication (CTA) such as independence-checking coding theory based CTA protocol proposed in [41] can be utilized.

C. Source to Relay

The transmitted signal from the source can be written as

$$\mathbf{x}_s^k = \underbrace{\mathbf{V}_s^k \mathbf{s}_s^k}_{=: \mathbf{v}_s^k} + \mathbf{e}_{t,s}^k, \quad (2)$$

where $\mathbf{s}_s^k \in \mathbb{C}^{d_s}$, $\mathbf{V}_s^k \in \mathbb{C}^{N_s \times d_s}$, and $\mathbf{e}_{t,s}^k \in \mathbb{C}^{N_s}$ represent the data symbol, the transmit precoding matrix and transmit distortion at the source, respectively. The number of data streams in each sub-carrier from the source is denoted by d_s and $\mathbb{E} \left\{ \mathbf{s}_s^k \mathbf{s}_s^{kH} \right\} = \mathbf{I}_{d_s}$. Furthermore, \mathbf{v}_s^k represents the desired signal to be transmitted from the source. Accordingly, the received signal at the relay can be written as

$$\mathbf{y}_r^k = \underbrace{\mathbf{H}_{sr}^k \mathbf{x}_s^k + \mathbf{H}_{rr}^k \mathbf{x}_r^k + \mathbf{n}_r^k}_{=: \mathbf{u}_r^k} + \mathbf{e}_{r,r}^k, \quad (3)$$

where $\mathbf{n}_r^k \sim \mathcal{CN}(\mathbf{0}_{M_r}, \sigma_{r,k}^2 \mathbf{I}_{M_r})$ and $\mathbf{e}_{r,r}^k$ are the noise and receiver distortion at the relay, respectively. Moreover, \mathbf{u}_r^k represents the intended (distortion-free) signal to be received at the relay. The distortion-free (known) part of the SI can be removed by applying a SIC technique [7], [9], [21]. The received signal after SIC⁴ can be stated as

$$\tilde{\mathbf{y}}_r^k = \mathbf{y}_r^k - \hat{\mathbf{H}}_{rr}^k \mathbf{V}_r^k \mathbf{s}_r^k = \hat{\mathbf{H}}_{sr}^k \mathbf{V}_s^k \mathbf{s}_s^k + \mathbf{v}_r^k, \quad (4)$$

where \mathbf{s}_r^k is the decoded signal at the relay and the collective interference-plus-noise at the relay can be represented as

$$\mathbf{v}_r^k = \hat{\mathbf{H}}_{sr}^k \mathbf{V}_s^k \mathbf{s}_s^k + \mathbf{H}_{sr}^k \mathbf{e}_{t,s}^k + \hat{\mathbf{H}}_{rr}^k \mathbf{V}_r^k \mathbf{s}_r^k + \mathbf{H}_{rr}^k \mathbf{e}_{t,r}^k + \mathbf{n}_r^k + \mathbf{e}_{r,r}^k. \quad (5)$$

The estimated signal vector at the relay can be obtained as

$$\tilde{\mathbf{s}}_s^k = \left(\mathbf{U}_r^k \right)^H \tilde{\mathbf{y}}_r^k, \quad (6)$$

where \mathbf{U}_r^k represents the linear receive filter at the relay.

⁴Please note that, here only the accurately known part of SI is subtracted from the received signal, i.e., the residual SI due to the CSI error and distortion remains in the system.

D. Relay to Destination

The transmitted signal from the relay can be written as

$$\mathbf{x}_r^k = \underbrace{\mathbf{V}_r^k \mathbf{s}_r^k}_{=: \mathbf{v}_r^k} + \mathbf{e}_{t,r}^k, \quad (7)$$

where $\mathbf{V}_r^k \in \mathbb{C}^{N_r \times d_r}$ and $\mathbf{e}_{t,r}^k \in \mathbb{C}^{N_r}$ represent the transmit precoding matrix and transmit distortion at the relay, respectively. The number of data streams in each sub-carrier from the relay is denoted by d_r and $\mathbb{E} \left\{ \mathbf{s}_r^k \mathbf{s}_r^{kH} \right\} = \mathbf{I}_{d_r}$. Moreover, \mathbf{v}_r^k represents the desired signal to be transmitted from the relay. Consequently, the signal received at the destination; including the interference from the source, can be written as

$$\begin{aligned} \mathbf{y}_d^k &= \underbrace{\mathbf{H}_{rd}^k \mathbf{x}_r^k + \mathbf{H}_{sd}^k \mathbf{x}_s^k + \mathbf{n}_d^k}_{=: \mathbf{u}_d^k} + \mathbf{e}_{r,d}^k \\ &= \mathbf{H}_{rd}^k \mathbf{V}_r^k \mathbf{s}_r^k + \mathbf{H}_{rd}^k \mathbf{e}_{t,r}^k + \mathbf{H}_{sd}^k \mathbf{V}_s^k \mathbf{s}_s^k + \mathbf{H}_{sd}^k \mathbf{e}_{t,s}^k + \mathbf{e}_{r,d}^k + \mathbf{n}_d^k, \end{aligned} \quad (8)$$

where $\mathbf{n}_d^k \sim \mathcal{CN}(\mathbf{0}_{M_d}, \sigma_{d,k}^2 \mathbf{I}_{M_d})$ and $\mathbf{e}_{r,d}^k$ are the noise and receiver distortion at the destination, respectively. Furthermore, \mathbf{u}_d^k represents the intended (distortion-free) signal to be received at the destination. The direct link is considered as an interference at the destination as its signal power is very weak (due to path loss). Accordingly, the collective interference-plus-noise at the destination can be stated as

$$\mathbf{v}_d^k = \tilde{\mathbf{H}}_{rd}^k \mathbf{V}_r^k \mathbf{s}_r^k + \mathbf{H}_{rd}^k \mathbf{e}_{t,r}^k + \mathbf{H}_{sd}^k \mathbf{V}_s^k \mathbf{s}_s^k + \mathbf{H}_{sd}^k \mathbf{e}_{t,s}^k + \mathbf{e}_{r,d}^k + \mathbf{n}_d^k. \quad (9)$$

The estimated signal vector at the destination can be obtained as

$$\tilde{\mathbf{s}}_r^k = \left(\mathbf{U}_d^k \right)^H \mathbf{y}_d^k, \quad (10)$$

where \mathbf{U}_r^k is the linear receive filter at the destination.

E. Limited Dynamic Range

The inaccuracies of hardware components such as ADC and digital to analog converter (DAC) error, noises caused by power amplifiers, automatic gain control (AGC) and oscillator on transmit and receive chains are jointly modelled for FD MIMO transceiver in [13], [39], based on [3], [42]–[44]. The hardware inaccuracies of the transmit (receive) chain for each antenna is jointly modelled as an additive distortion and can be expressed as

$$\begin{aligned} x_l(t) &= v_l(t) + e_{l,t}(t) \\ y_l(t) &= u_l(t) + e_{r,l}(t), \end{aligned} \quad (11)$$

such that,

$$\begin{aligned} e_{l,t}(t) &\sim \mathcal{CN}(0, \kappa_l \mathbb{E}\{|v_l(t)|^2\}), e_{r,l}(t) \sim \mathcal{CN}(0, \beta_l \mathbb{E}\{|u_l(t)|^2\}), \\ e_{l,t}(t) &\perp v_l(t), e_{l,t}(t) \perp e_{l,t'}(t), e_{l,t}(t) \perp e_{l,t}(t'), l \neq l', t \neq t' \\ e_{r,l}(t) &\perp u_l(t), e_{r,l}(t) \perp e_{r,l'}(t), e_{r,l}(t) \perp e_{r,l}(t'), l \neq l', t \neq t', \end{aligned} \quad (12)$$

i.e., the distortion terms are proportional to the intensity of the intended signals. In the equations (11) and (12), t denotes the instance of time, and $v_l(u)$, $x_l(y)$, and $e_{l,t}(e_{r,l})$ are respectively the baseband time-domain representation of the intended transmit (receive) signal, the actual transmit (receive) signal, and the additive transmit (receive) distortion at the l -th transmit (receive) chain. The κ_l and β_l are the distortion coefficient for the l -th transmit and receive chain, respectively.

In [12], we discuss the characterization of the impact of these hardware distortions in the frequency domain for an

OFDM system. In this work, we extend this characterization in the frequency domain to a general MC strategy, where the sub-carriers k are orthogonal to each other with a unitary linear transformation, for example OVFSF-CDMA, OFDM and cyclic-prefix (CP)-OFDM. Let \mathbf{Q} be a $K \times K$ unitary transformation matrix, where the columns of the matrix \mathbf{Q} represent the basis of the generalized sub-carrier waveforms which are orthonormal to each other. The total number of sub-carriers is K . NT_s is the duration of one communication block, where T_s is the sample period.

The unitary transformation representation of the sampled time domain signal for each communication block can be written as

$$\begin{aligned} x_l^k &= \sum_{n=0}^{N-1} x_l(nT_s)q_{k,n}^* = \underbrace{\sum_{n=0}^{N-1} v_l(nT_s)q_{k,n}^*}_{=:v_l^k} + \underbrace{\sum_{n=0}^{N-1} e_{\text{tx}_l}(nT_s)q_{k,n}^*}_{=:e_{t,l}^k} \\ y_l^k &= \sum_{n=0}^{N-1} y_l(nT_s)q_{k,n}^* = \underbrace{\sum_{n=0}^{N-1} u_l(nT_s)q_{k,n}^*}_{=:u_l^k} + \underbrace{\sum_{n=0}^{N-1} e_{\text{rx}_l}(nT_s)q_{k,n}^*}_{=:e_{r,l}^k} \end{aligned} \quad (13)$$

where $q_{k,n}$ is the element of the unitary matrix \mathbf{Q} at the k -th row and n -th column.

Lemma II.1. *Let us define \tilde{x}_l^m and \tilde{y}_l^m as the intended transmit and receive signal via m -th sub-carrier at the l -th transmit/receive chain. The impact of hardware distortions in the unitary transformed domain is characterized as*

$$e_{t,l}^k \sim \mathcal{CN}\left(0, \frac{\tilde{\kappa}_l}{K} \sum_{m=1}^K \mathbb{E}\left\{|\tilde{y}_l^m|^2\right\}\right), \quad e_{t,l}^k \perp \tilde{y}_l^k, \quad e_{t,l}^k \perp e_{t,l'}^k, \quad (14)$$

$$e_{r,l}^k \sim \mathcal{CN}\left(0, \frac{\tilde{\beta}_l}{K} \sum_{m=1}^K \mathbb{E}\left\{|\tilde{x}_l^m|^2\right\}\right), \quad e_{r,l}^k \perp \tilde{x}_l^k, \quad e_{r,l}^k \perp e_{r,l'}^k, \quad (15)$$

transforming the statistical independence, as well as the proportional variance properties from the time domain. Here, K represents the total number of sub-carriers. $\tilde{\kappa}_l$ and $\tilde{\beta}_l$ correspond to the transmit and receive distortion coefficient at the l -th transmit/receive chain.

Proof: Please refer to the Appendix. \blacksquare

Following the lemma II.1, the statistics of the distortion terms can be written as

$$\mathbf{e}_{t,s}^k \sim \mathcal{CN}\left(\mathbf{0}_{N_s}, \frac{1}{K} \tilde{\Theta}_{\text{tx},s} \mathbf{P}_{\text{tx},s}\right), \quad (16)$$

$$\mathbf{e}_{t,r}^k \sim \mathcal{CN}\left(\mathbf{0}_{N_r}, \frac{1}{K} \tilde{\Theta}_{\text{tx},r} \mathbf{P}_{\text{tx},r}\right), \quad (17)$$

$$\mathbf{e}_{r,r}^k \sim \mathcal{CN}\left(\mathbf{0}_{M_r}, \frac{1}{K} \tilde{\Theta}_{\text{rx},r} \mathbf{P}_{\text{rx},r}\right), \quad (18)$$

$$\mathbf{e}_{r,d}^k \sim \mathcal{CN}\left(\mathbf{0}_{M_d}, \frac{1}{K} \tilde{\Theta}_{\text{rx},d} \mathbf{P}_{\text{rx},d}\right), \quad (19)$$

where

$$\mathbf{P}_{\text{tx},s} := \sum_{k \in \mathbb{K}} \text{diag}\left(\mathbb{E}\left\{\mathbf{v}_s^k \left(\mathbf{v}_s^k\right)^H\right\}\right), \quad (20)$$

$$\mathbf{P}_{\text{tx},r} := \sum_{k \in \mathbb{K}} \text{diag}\left(\mathbb{E}\left\{\mathbf{v}_r^k \left(\mathbf{v}_r^k\right)^H\right\}\right), \quad (21)$$

$$\mathbf{P}_{\text{rx},r} := \sum_{k \in \mathbb{K}} \text{diag}\left(\mathbb{E}\left\{\mathbf{u}_r^k \left(\mathbf{u}_r^k\right)^H\right\}\right), \quad (22)$$

$$\mathbf{P}_{\text{rx},d} := \sum_{k \in \mathbb{K}} \text{diag}\left(\mathbb{E}\left\{\mathbf{u}_d^k \left(\mathbf{u}_d^k\right)^H\right\}\right), \quad (23)$$

where $\tilde{\Theta}_{\text{tx},s}$ and $\tilde{\Theta}_{\text{tx},r}$ ($\tilde{\Theta}_{\text{rx},r}$ and $\tilde{\Theta}_{\text{rx},d}$) are diagonal matrices consisting of transmit (receive) distortion coefficients for the corresponding chains. Correspondingly, $\mathbf{P}_{\text{tx},s}$ and $\mathbf{P}_{\text{tx},r}$ ($\mathbf{P}_{\text{rx},r}$ and $\mathbf{P}_{\text{rx},d}$) are the diagonal matrices including intended transmit (receive) signal power at the corresponding chains. Let us define $\Theta_{\text{tx},r} = \frac{1}{K} \tilde{\Theta}_{\text{tx},r}$, $\Theta_{\text{tx},s} = \frac{1}{K} \tilde{\Theta}_{\text{tx},s}$, $\Theta_{\text{rx},r} = \frac{1}{K} \tilde{\Theta}_{\text{rx},r}$, and $\Theta_{\text{rx},d} = \frac{1}{K} \tilde{\Theta}_{\text{rx},d}$ for further calculations.

F. Mean-Squared Error (MSE) Matrix

Considering \mathbf{V}_s^k and \mathbf{U}_r^k as the linear source transmit precoder and relay receive filters at the sub-carrier k , the MSE matrix for the source-relay system can be defined as

$$\begin{aligned} \mathbf{E}_r^k &= \mathbf{E}\left\{\left(\tilde{\mathbf{s}}_s^k - \mathbf{s}_s^k\right)\left(\tilde{\mathbf{s}}_s^k - \mathbf{s}_s^k\right)^H\right\} \\ &= \left(\left(\mathbf{U}_r^k\right)^H \hat{\mathbf{H}}_{\text{sr}}^k \mathbf{V}_s^k - \mathbf{I}_{d_s}\right) \left(\left(\mathbf{U}_r^k\right)^H \hat{\mathbf{H}}_{\text{sr}}^k \mathbf{V}_s^k - \mathbf{I}_{d_s}\right)^H \\ &\quad + \left(\mathbf{U}_r^k\right)^H \Sigma_r^k \mathbf{U}_r^k, \end{aligned} \quad (24)$$

where Σ_r^k is the covariance of the received collective interference-plus-noise signal at the relay and can be obtained as in (25) for $k \in \mathbb{K}$. Similarly, the MSE matrix for the relay-destination system considering \mathbf{V}_r^k and \mathbf{U}_d^k as the linear relay transmit precoder and destination receive filters at the sub-carrier k can be obtained as

$$\begin{aligned} \mathbf{E}_d^k &= \mathbf{E}\left\{\left(\tilde{\mathbf{s}}_r^k - \mathbf{s}_r^k\right)\left(\tilde{\mathbf{s}}_r^k - \mathbf{s}_r^k\right)^H\right\} \\ &= \left(\left(\mathbf{U}_d^k\right)^H \hat{\mathbf{H}}_{\text{rd}}^k \mathbf{V}_r^k - \mathbf{I}_{d_r}\right) \left(\left(\mathbf{U}_d^k\right)^H \hat{\mathbf{H}}_{\text{rd}}^k \mathbf{V}_r^k - \mathbf{I}_{d_r}\right)^H \\ &\quad + \left(\mathbf{U}_d^k\right)^H \Sigma_d^k \mathbf{U}_d^k. \end{aligned} \quad (26)$$

where Σ_d^k , the covariance of the interference-plus-noise signal at the destination, can be expressed as in (27) for $k \in \mathbb{K}$. In (25) and (27), we ignore the higher-order terms of the transmit and receive distortion since the transmit and receive distortion coefficients of each transmit/receive chains ($\tilde{\kappa}_l/\tilde{\beta}_l$) lie within the range of 0 and 1 and mostly have very small values.

III. LINEAR PRECODER AND DECODER DESIGN: AN AQCP FRAMEWORK

In this section, we discuss the linear transceiver design problem of an FD MIMO DF relay system for sum-rate maximization, power minimization and energy efficiency maximization.

$$\begin{aligned}
\Sigma_r^k &= \mathbb{E} \left\{ \mathbf{v}_r^k \mathbf{v}_r^{kH} \right\} \approx \underbrace{\widehat{\mathbf{H}}_{sr}^k \Theta_{tx,s} \text{diag} \left(\sum_{l \in \mathbb{K}} \mathbf{v}_s^l (\mathbf{v}_s^l)^H \right) (\widehat{\mathbf{H}}_{sr}^k)^H + \mathbf{D}_{sr}^k \text{Tr} \left(\Theta_{tx,s} \text{diag} \left(\sum_{l \in \mathbb{K}} \mathbf{v}_s^l (\mathbf{v}_s^l)^H \right) \right)}_{\text{Source transmit distortion}} + \underbrace{\sigma_{r,k}^2 \mathbf{I}_{M_r}}_{\text{Thermal noise}} \\
&+ \underbrace{\widehat{\mathbf{H}}_{rr}^k \Theta_{tx,r} \text{diag} \left(\sum_{l \in \mathbb{K}} \mathbf{v}_r^l (\mathbf{v}_r^l)^H \right) (\widehat{\mathbf{H}}_{rr}^k)^H + \mathbf{D}_{rr}^k \text{Tr} \left(\Theta_{tx,r} \text{diag} \left(\sum_{l \in \mathbb{K}} \mathbf{v}_r^l (\mathbf{v}_r^l)^H \right) \right)}_{\text{Relay transmit distortion}} + \underbrace{\mathbf{D}_{sr}^k \text{Tr} \left(\mathbf{v}_s^k (\mathbf{v}_s^k)^H \right) + \mathbf{D}_{rr}^k \text{Tr} \left(\mathbf{v}_r^k (\mathbf{v}_r^k)^H \right)}_{\text{CSI error in source-relay and relay SI channel}} \\
&+ \underbrace{\Theta_{rx,r} \text{diag} \left(\sum_{l \in \mathbb{K}} \left(\widehat{\mathbf{H}}_{sr}^l \mathbf{v}_s^l (\mathbf{v}_s^l)^H (\widehat{\mathbf{H}}_{sr}^l)^H + \mathbf{D}_{sr}^l \text{Tr} \left(\mathbf{v}_s^l (\mathbf{v}_s^l)^H \right) \right) \right)}_{\text{Relay receive distortion}} + \underbrace{\sum_{l \in \mathbb{K}} \left(\widehat{\mathbf{H}}_{rr}^l \mathbf{v}_r^l (\mathbf{v}_r^l)^H (\widehat{\mathbf{H}}_{rr}^l)^H + \mathbf{D}_{rr}^l \text{Tr} \left(\mathbf{v}_r^l (\mathbf{v}_r^l)^H \right) + \sigma_{r,l}^2 \mathbf{I}_{M_r} \right)}_{\text{Relay receive distortion}}. \tag{25}
\end{aligned}$$

$$\begin{aligned}
\Sigma_d^k &= \mathbb{E} \left\{ \mathbf{v}_d^k \mathbf{v}_d^{kH} \right\} \approx \underbrace{\widehat{\mathbf{H}}_{rd}^k \Theta_{tx,r} \text{diag} \left(\sum_{l \in \mathbb{K}} \mathbf{v}_r^l (\mathbf{v}_r^l)^H \right) (\widehat{\mathbf{H}}_{rd}^k)^H + \mathbf{D}_{rd}^k \text{Tr} \left(\Theta_{tx,r} \text{diag} \left(\sum_{l \in \mathbb{K}} \mathbf{v}_r^l (\mathbf{v}_r^l)^H \right) \right)}_{\text{Relay transmit distortion}} + \underbrace{\mathbf{D}_{rd}^k \text{Tr} \left(\mathbf{v}_r^k (\mathbf{v}_r^k)^H \right)}_{\text{CSI error in relay-destination channel}} + \underbrace{\sigma_{d,k}^2 \mathbf{I}_{M_d}}_{\text{Thermal noise}} \\
&+ \underbrace{\widehat{\mathbf{H}}_{sd}^k \Theta_{tx,s} \text{diag} \left(\sum_{l \in \mathbb{K}} \mathbf{v}_s^l (\mathbf{v}_s^l)^H \right) (\widehat{\mathbf{H}}_{sd}^k)^H + \mathbf{D}_{sd}^k \text{Tr} \left(\Theta_{tx,s} \text{diag} \left(\sum_{l \in \mathbb{K}} \mathbf{v}_s^l (\mathbf{v}_s^l)^H \right) \right)}_{\text{Source transmit distortion}} + \underbrace{\widehat{\mathbf{H}}_{sd}^k \mathbf{v}_s^k (\mathbf{v}_s^k)^H (\widehat{\mathbf{H}}_{sd}^k)^H + \mathbf{D}_{sd}^k \text{Tr} \left(\mathbf{v}_s^k (\mathbf{v}_s^k)^H \right)}_{\text{Interference from Source}} \\
&+ \underbrace{\Theta_{rx,d} \text{diag} \left(\sum_{l \in \mathbb{K}} \left(\widehat{\mathbf{H}}_{rd}^l \mathbf{v}_r^l (\mathbf{v}_r^l)^H (\widehat{\mathbf{H}}_{rd}^l)^H + \mathbf{D}_{rd}^l \text{Tr} \left(\mathbf{v}_r^l (\mathbf{v}_r^l)^H \right) \right) \right)}_{\text{Destination receive distortion}} + \underbrace{\sum_{l \in \mathbb{K}} \left(\widehat{\mathbf{H}}_{sd}^l \mathbf{v}_s^l (\mathbf{v}_s^l)^H (\widehat{\mathbf{H}}_{sd}^l)^H + \mathbf{D}_{sd}^l \text{Tr} \left(\mathbf{v}_s^l (\mathbf{v}_s^l)^H \right) + \sigma_{d,l}^2 \mathbf{I}_{M_d} \right)}_{\text{Destination receive distortion}}. \tag{27}
\end{aligned}$$

A. Rate Maximization

In recent years, due to the scarcity of spectrum resource, spectral efficiency has become one of the most necessitous factors in wireless communications. Here, we consider spectral efficiency in terms of sum-rate maximization. The achievable sum-rate of a relay system is the minimum achievable sum-rate between the source-relay link and relay-destination link. The sum-rate maximization problem for the relay system can be hence formulated⁵ as

$$\text{maximize}_{\mathbb{V}_s, \mathbb{V}_r} \min \{R_{sr}, R_{rd}\} \tag{28a}$$

$$\text{subject to} \quad \text{Tr} \left((\mathbf{I}_{N_s} + \Theta_{tx,s}) \sum_{l \in \mathbb{K}} \mathbf{v}_s^l \mathbf{v}_s^{lH} \right) \leq P_{s,\max}, \tag{28b}$$

$$\text{Tr} \left((\mathbf{I}_{N_r} + \Theta_{tx,r}) \sum_{l \in \mathbb{K}} \mathbf{v}_r^l \mathbf{v}_r^{lH} \right) \leq P_{r,\max}, \tag{28c}$$

where $\mathbb{V}_{\mathcal{X}} := \mathbf{V}_{\mathcal{X}}^k, k \in \mathbb{K}$ with $\mathcal{X} \in \{s, r\}$ and $\mathbb{U}_{\mathcal{Y}} := \mathbf{U}_{\mathcal{Y}}^k, k \in \mathbb{K}$ with $\mathcal{Y} \in \{r, d\}$. The total sum-rate between the source and relay, and the relay and destination are denoted by R_{sr} and R_{rd} , respectively. $P_{s,\max}$ and $P_{r,\max}$ denote the maximum affordable transmit power at the source and the relay, respectively. Subsequently, the rate functions can be

⁵Please note that the achievable rate expressions for the studied FD relaying channel, indicating the Shannon bound on the error-free communication hold assuming a sufficiently long coding block, the Gaussian transmit signal codeword, as well as the Gaussian distribution of noise, CSI error and the transmit and received signal impairments [13], [39].

defined as

$$\begin{aligned}
R_{sr} &= \gamma_0 \sum_{k \in \mathbb{K}} R_{sr}^k \\
&= \gamma_0 \sum_{k \in \mathbb{K}} \log_2 \left| \mathbf{I}_{d_s} + (\mathbf{v}_s^k)^H (\widehat{\mathbf{H}}_{sr}^k)^H (\Sigma_r^k)^{-1} \widehat{\mathbf{H}}_{sr}^k \mathbf{v}_s^k \right|
\end{aligned}$$

and

$$\begin{aligned}
R_{rd} &= \gamma_0 \sum_{k \in \mathbb{K}} R_{rd}^k \\
&= \gamma_0 \sum_{k \in \mathbb{K}} \log_2 \left| \mathbf{I}_{d_r} + (\mathbf{v}_r^k)^H (\widehat{\mathbf{H}}_{rd}^k)^H (\Sigma_d^k)^{-1} \widehat{\mathbf{H}}_{rd}^k \mathbf{v}_r^k \right|,
\end{aligned}$$

where $\gamma_0 = (T_{\text{tot}} - T_{\text{train}})/T_{\text{tot}}$ represents the fraction of time interval allocated for the data transmission. The optimization problem (28) can be reformulated as

$$\begin{aligned}
&\text{maximize}_{\mathbb{V}_s, \mathbb{V}_r} \sum_{k \in \mathbb{K}} t_k \\
&\text{subject to} \quad R_{sr}^k \geq t_k, \quad R_{rd}^k \geq t_k, \\
&\quad\quad\quad (28b), (28c).
\end{aligned} \tag{29}$$

where t_k are auxiliary variables introduced to transfer parts of the problem objective in (28) into the constraint sets in (29). It can be observed that the problem (29) is not a convex optimization problem. In the following, we apply the known WMMSE method [45] to facilitate a convergent alternating optimization.

We can write the optimal MMSE receive filter at the relay

as

$$\mathbf{U}_{r,\text{mmse}}^k = \left(\boldsymbol{\Sigma}_r^k + \widehat{\mathbf{H}}_{\text{sr}}^k \mathbf{V}_s^k \left(\mathbf{V}_s^k \right)^H \left(\widehat{\mathbf{H}}_{\text{sr}}^k \right)^H \right)^{-1} \widehat{\mathbf{H}}_{\text{sr}}^k \mathbf{V}_s^k \quad (30)$$

and at the destination as

$$\mathbf{U}_{d,\text{mmse}}^k = \left(\boldsymbol{\Sigma}_d^k + \widehat{\mathbf{H}}_{\text{rd}}^k \mathbf{V}_r^k \left(\mathbf{V}_r^k \right)^H \left(\widehat{\mathbf{H}}_{\text{rd}}^k \right)^H \right)^{-1} \widehat{\mathbf{H}}_{\text{rd}}^k \mathbf{V}_r^k. \quad (31)$$

By applying (30) and (31) in (24) and (26), we get,

$$\mathbf{E}_{r,\text{mmse}}^k = \left(\mathbf{I}_{d_s} + \left(\mathbf{V}_s^k \right)^H \left(\widehat{\mathbf{H}}_{\text{sr}}^k \right)^H \left(\boldsymbol{\Sigma}_r^k \right)^{-1} \widehat{\mathbf{H}}_{\text{sr}}^k \mathbf{V}_s^k \right)^{-1}, \quad (32)$$

$$\mathbf{E}_{d,\text{mmse}}^k = \left(\mathbf{I}_{d_r} + \left(\mathbf{V}_r^k \right)^H \left(\widehat{\mathbf{H}}_{\text{rd}}^k \right)^H \left(\boldsymbol{\Sigma}_d^k \right)^{-1} \widehat{\mathbf{H}}_{\text{rd}}^k \mathbf{V}_r^k \right)^{-1}. \quad (33)$$

Using (32) and (33), the rate functions can be written as

$$R_{\text{sr}}^k = -\gamma_0 \log_2 \left| \mathbf{E}_{r,\text{mmse}}^k \right|, \quad (34)$$

$$R_{\text{rd}}^k = -\gamma_0 \log_2 \left| \mathbf{E}_{d,\text{mmse}}^k \right|. \quad (35)$$

Lemma III.1. [12, lemma III.1.] [46, lemma 2] Let $\mathbf{E} \in \mathbb{C}^{d \times d}$ be a positive definite matrix. The maximization of the term $-\log|\mathbf{E}|$ is equivalent to the maximization

$$\max_{\mathbf{E}, \mathbf{S}} -\text{Tr}(\mathbf{S}\mathbf{E}) + \log|\mathbf{S}| + d \quad (36)$$

where $\mathbf{S} \in \mathbb{C}^{d \times d}$ is a positive definite matrix, and we have

$$\mathbf{S} = \mathbf{E}^{-1}, \quad (37)$$

at the optimality.

By using the Lemma III.1, the optimization problem (29) can be written as

$$\max_{\mathbb{V}_s, \mathbb{U}_r, \mathbb{S}_r, \mathbb{V}_r, \mathbb{U}_d, \mathbb{S}_d} \sum_{k \in \mathbb{K}} t_k \quad (38a)$$

$$\text{subject to} \quad -\text{Tr}(\mathbf{S}_r^k \mathbf{E}_r^k) + \log|\mathbf{S}_r^k| + d_s \geq t_k, \quad (38b)$$

$$-\text{Tr}(\mathbf{S}_d^k \mathbf{E}_d^k) + \log|\mathbf{S}_d^k| + d_r \geq t_k, \quad (38c)$$

(28b), (28c),

where $\mathbb{S}_y := \mathbf{S}_y^k \succ 0, k \in \mathbb{K}$ with $\mathcal{Y} \in \{\text{r}, \text{d}\}$. Please note that the obtained problem is not a jointly convex problem. However, it is a quadratic convex program over \mathbb{V}_s and \mathbb{V}_r , when other variables are fixed. Moreover, the optimization over \mathbb{U}_r and \mathbb{U}_d can be obtained from (30) and (31), respectively. Whereas, the optimization over \mathbb{S}_r and \mathbb{S}_d can be acquired using (32) and (33), as $\mathbf{S}_r^k = \mathbf{E}_r^k{}^{-1}$ and $\mathbf{S}_d^k = \mathbf{E}_d^k{}^{-1}$. This facilitates an alternating optimization, where in each step the corresponding problem is solved to optimality. Due to the monotonic increase of the objective in each step and the fact that the system sum-rate is bounded from above, the alternating optimization steps lead to convergence. Algorithm 1 defines the detailed procedure.

1) *Joint carrier (JC) decoding and remapping:* In this section, we consider the optimization constraints over all the sub-carriers jointly. This way, we can take advantage of the MC system, by allowing the relay system to decode the signal from one sub-carrier and forward it to the destination through another sub-carrier, thereby improving the system in terms of total sum-rate. Accordingly, the sum-rate optimization problem

Algorithm 1 AQCP-WMMSE design for sum-rate maximization

- 1: $a \leftarrow 0$ (set iteration number to zero)
 - 2: $\mathbb{V}_s, \mathbb{V}_r \leftarrow$ right singular matrix initialization [47, Appendix A]
 - 3: **repeat**
 - 4: $a \leftarrow a + 1$
 - 5: $\mathbb{U}_r, \mathbb{U}_d \leftarrow$ solve (30) and (31), respectively
 - 6: $\mathbb{S}_r, \mathbb{S}_d \leftarrow \mathbf{S}_r^k = \mathbf{E}_r^k{}^{-1}$ and $\mathbf{S}_d^k = \mathbf{E}_d^k{}^{-1}$, respectively
 - 7: $\mathbb{V}_s, \mathbb{V}_r \leftarrow$ solve (38), with fixed $\mathbb{U}_r, \mathbb{U}_d, \mathbb{S}_r$, and \mathbb{S}_d
 - 8: **until** a stable point, or maximum number of a reached
 - 9: **return** $\{\mathbb{V}_s, \mathbb{V}_r\}$
-

with joint-carrier decoding and remapping can be defined as

$$\begin{aligned} & \max_{\mathbb{V}_s, \mathbb{V}_r, \mathbb{U}_r, \mathbb{U}_d, \mathbb{S}_r, \mathbb{S}_d} t \\ & \text{subject to} \quad \sum_{k \in \mathbb{K}} \left(-\text{Tr}(\mathbf{S}_r^k \mathbf{E}_r^k) + \log|\mathbf{S}_r^k| + d_s \right) \geq t, \\ & \quad \quad \quad \sum_{k \in \mathbb{K}} \left(-\text{Tr}(\mathbf{S}_d^k \mathbf{E}_d^k) + \log|\mathbf{S}_d^k| + d_r \right) \geq t, \end{aligned} \quad (39)$$

(28b), (28c).

Alternating quadratic convex program steps that are applied to (38) can be used to solve the above optimization problem (39).

B. Power Minimization

In this section, our goal is to attain a design that minimizes the total power consumption for a guaranteed pre-defined rate requirement γ . The total power consumption P_{tot} can be defined as

$$P_{\text{tot}} = P_s + P_r, \quad (40)$$

where

$$P_s = \frac{1}{\mu_s} \sum_{k \in \mathbb{K}} \mathbb{E}\{\|\mathbf{x}_s^k\|^2\} + P_{s_{\text{zero}}}, \quad (41)$$

$$P_r = \frac{1}{\mu_r} \sum_{k \in \mathbb{K}} \mathbb{E}\{\|\mathbf{x}_r^k\|^2\} + P_{r_{\text{zero}}} + P_{\text{FD}},$$

where μ_s and μ_r are the efficiencies of the power amplifier at the source and relay, respectively. $P_{s_{\text{zero}}}$ and $P_{r_{\text{zero}}}$ are the power dissipated by other circuit blocks at the transmitter chain of source and relay, respectively. P_{FD} is the power required for SIC. By using the above definition, the total power minimization problem can be expressed as

$$\min_{\mathbb{V}_s, \mathbb{V}_r} P_{\text{tot}} \quad (42a)$$

$$\text{subject to} \quad P_s \leq P_{s,\text{max}}, \quad P_r \leq P_{r,\text{max}}, \quad (42b)$$

$$\min\{R_{\text{sr}}, R_{\text{rd}}\} \geq \gamma. \quad (42c)$$

The above problem can be solved using alternating quadratic convex programming steps similar to (39). However, the initialization of the variable \mathbb{V}_s and \mathbb{V}_r must belong to the feasible set of the problem. In order to find a feasible initialization point, we need to solve the following optimization problem,

$$\min_{\mathbb{V}_s, \mathbb{V}_r} \varepsilon \quad (43a)$$

$$\text{subject to} \quad P_s \leq P_{s,\text{max}}, \quad P_r \leq P_{r,\text{max}}, \quad (43b)$$

$$R_{\text{sr}} + \varepsilon \geq \gamma, \quad R_{\text{rd}} + \varepsilon \geq \gamma, \quad \varepsilon \geq 0. \quad (43c)$$

The solution to the above problem is obtained by an alternating one similar to (39), and can be used as the initialization point for (42). Algorithm 2 defines the detailed procedure.

Algorithm 2 AQCP-WMMSE design for power minimization

```

1:  $a \leftarrow 0$  (set iteration number to zero)
2:  $\mathbb{V}_s, \mathbb{V}_r \leftarrow$  solve (43)
3: repeat
4:    $a \leftarrow a + 1$ 
5:    $\mathbb{U}_r, \mathbb{U}_d \leftarrow$  solve (30) and (31), respectively
6:    $\mathbb{S}_r, \mathbb{S}_d \leftarrow \mathbf{S}_r^k = \mathbf{E}_r^{k-1}$  and  $\mathbf{S}_d^k = \mathbf{E}_d^{k-1}$ , respectively
7:    $\mathbb{V}_s, \mathbb{V}_r \leftarrow$  solve (42), with fixed  $\mathbb{U}_r, \mathbb{U}_d, \mathbb{S}_r$ , and  $\mathbb{S}_d$ 
8: until a stable point, or maximum number of  $a$  reached
9: return  $\{\mathbb{V}_s, \mathbb{V}_r\}$ 

```

Algorithm 3 AQCP-WMMSE design for energy efficiency maximization

```

1:  $a \leftarrow 0$  (set iteration number to zero)
2:  $\mathbb{V}_s, \mathbb{V}_r \leftarrow$  right singular matrix initialization [47, Appendix A]
3: repeat
4:    $a \leftarrow a + 1$ 
5:    $\mathbb{U}_r, \mathbb{U}_d \leftarrow$  solve (30) and (31), respectively
6:    $\mathbb{S}_r, \mathbb{S}_d \leftarrow \mathbf{S}_r^k = \mathbf{E}_r^{k-1}$  and  $\mathbf{S}_d^k = \mathbf{E}_d^{k-1}$ , respectively
7:    $\lambda \leftarrow$  solve (47)
8:    $\mathbb{V}_s, \mathbb{V}_r \leftarrow$  solve (46), with fixed  $\mathbb{U}_r, \mathbb{U}_d, \mathbb{S}_r, \mathbb{S}_d$ , and  $\lambda$ 
9: until a stable point, or maximum number of  $a$  reached
10: return  $\{\mathbb{V}_s, \mathbb{V}_r\}$ 

```

C. Energy Efficiency Maximization

The main idea behind energy efficiency is to perform the same amount of tasks utilizing less energy. Eliminating energy waste also provides economic benefits and ecological sustainability. Therefore, energy-efficient or green technologies have gained more attention in designing a future wireless system. In this section, the energy efficiency is defined as the ratio of the system sum-rate to the total power consumption of both the source and the relay. The energy efficiency maximization problem can be expressed as

$$\underset{\mathbb{V}_s, \mathbb{V}_r}{\text{maximize}} \quad t/P_{\text{tot}} \quad (44a)$$

$$\text{subject to} \quad P_s \leq P_{s,\text{max}}, \quad P_r \leq P_{r,\text{max}}, \quad (44b)$$

$$\min\{R_{\text{sr}}, R_{\text{rd}}\} \geq t. \quad (44c)$$

Using the similar approach of sum-rate maximization problem, the above optimization (44) can also be written as

$$\underset{\mathbb{V}_s, \mathbb{U}_r, \mathbb{V}_r, \mathbb{S}_r, \mathbb{U}_d, \mathbb{S}_d}{\text{maximize}} \quad t/P_{\text{tot}} \quad (45a)$$

$$\text{subject to} \quad P_s \leq P_{s,\text{max}}, \quad P_r \leq P_{r,\text{max}}, \quad (45b)$$

$$\sum_{k \in \mathbb{K}} (-\text{Tr}(\mathbf{S}_r^k \mathbf{E}_r^k) + \log|\mathbf{S}_r^k| + d_s) \geq t, \quad (45c)$$

$$\sum_{k \in \mathbb{K}} (-\text{Tr}(\mathbf{S}_d^k \mathbf{E}_d^k) + \log|\mathbf{S}_d^k| + d_r) \geq t. \quad (45d)$$

Using Dinkelbach's algorithm [48], we can rewrite the optimization problem as

$$\underset{\mathbb{V}_s, \mathbb{U}_r, \mathbb{V}_r, \mathbb{S}_r, \mathbb{U}_d, \mathbb{S}_d, \lambda}{\text{maximize}} \quad t - \lambda P_{\text{tot}} \quad (46a)$$

$$\text{subject to} \quad P_s \leq P_{s,\text{max}}, \quad P_r \leq P_{r,\text{max}}, \quad (46b)$$

$$\sum_{k \in \mathbb{K}} (-\text{Tr}(\mathbf{S}_r^k \mathbf{E}_r^k) + \log|\mathbf{S}_r^k| + d_s) \geq t, \quad (46c)$$

$$\sum_{k \in \mathbb{K}} (-\text{Tr}(\mathbf{S}_d^k \mathbf{E}_d^k) + \log|\mathbf{S}_d^k| + d_r) \geq t. \quad (46d)$$

For fixed \mathbb{V}_s and \mathbb{V}_r , the MMSE filters and the MMSE error matrix can be calculated from (30), (31), and (32), (33) respectively. The λ can be determined from

$$t - \lambda P_{\text{tot}} = 0, \quad (47)$$

where \mathbb{V}_s and \mathbb{V}_r are updated by solving (46) with fixed $\mathbb{U}_r, \mathbb{U}_d, \mathbb{S}_r, \mathbb{S}_d$ and λ . The optimization problem is solved until a stable point is reached. Since the objective increase monotonically and it is bounded from above, we can conclude that a global optimal value can be achieved. Algorithm 3 defines the detailed algorithm procedure.

IV. COMPUTATIONAL COMPLEXITY

In this section, we evaluate the arithmetic computational complexity corresponding to Algorithm 1. In this algorithm, the consideration of the impact of hardware distortions and CSI error escalates the problem dimension and also adds complexity to the optimization problem structure.

The optimization variables $\mathbb{U}_r, \mathbb{U}_d, \mathbb{S}_r$ and \mathbb{S}_d are obtained using their closed-form solution. Therefore, the computational complexity is dominated by the calculation of the variables $\mathbb{V}_s, \mathbb{V}_r$ and t_k . The optimization problem over $\mathbb{V}_s, \mathbb{V}_r$ and t_k can be cast as a conic quadratic program (CQP). The general CQP can be stated as

$$\min_{\mathbf{x}} \{ \mathbf{c}^T \mathbf{x} : \|\mathbf{A}_i \mathbf{x} + \mathbf{b}_i\|_2 \leq \mathbf{c}_i^T \mathbf{x} + \mathbf{d}_i, i = 1, 2, \dots, m; \|\mathbf{x}\| \leq R \},$$

for $\mathbf{x} \in \mathbb{R}^n, \mathbf{b}_i \in \mathbb{R}^{k_i}$. For the definition of problem structure; please refer to [49, Section 4.6.2]. The arithmetic complexity for attaining an ε -solution to the above problem is upper bounded by

$$\mathcal{O}(1)(m+1)^{\frac{1}{2}} n(n^2 + m + \sum_{i=0}^m (k_i)^2) \text{digit}(\varepsilon),$$

where $\mathcal{O}(1)$ is a positive constant, and $\text{digit}(\varepsilon)$ corresponds to the required solution precision [49, Section 4.6.2]. The computation necessary for each step depends on the size of the variable space (n), the number of constraints (m) and their corresponding block size (k_i). For our problem, the size of the variable space is given as $n = K(2(N_s + N_r) + 1)$. The block size for each constraint, $k_i = 2(d_s^2(1 + 2KN_s) + 2KN_r d_s d_r + KN_s d_s + KN_r d_r + 2K + 2)$ corresponding to constraint (38b), as $k_i = 2(d_r^2(1 + 2KN_r) + (2KN_s + 1)d_s d_r + KN_s d_s + KN_r d_r + 2K + 2)$ corresponding to constraint (38c), furthermore $k_i = 2KN_s d_s$ belongs to power constraint (28b) and $k_i = 2KN_r d_r$ belongs to constraint (28c). The total number of constraints can be concluded to be $m = 2K + 2$.

For the joint decoding and mapping scenario, the size of the variable space changes to $n = 2K(N_s + N_r) + 1$. The number of constraints will be reduced to $m = 4$, where the block size for each constraint increases by K fold. As a remark, the actual computation load may differ from the above mentioned, as it depends on the utilized numerical solver and other structure simplification methods.

V. SIMULATION RESULTS

In this section, we evaluate the performance of the proposed transceiver design JC and PC introduced in Section III-C in

terms of sum-rate and energy efficiency for an FD MIMO OFDM DF relay system under various system conditions. All communication channels follow an uncorrelated Rayleigh flat fading model. The SI channel follows the characterization reported in [3]:

$$\mathbf{H}_{rr} \sim \mathcal{CN} \left(\sqrt{\frac{\rho_{si} K_R}{1 + K_R}} \mathbf{H}_0, \frac{\rho_{si}}{1 + K_R} \mathbf{I}_{M_r} \otimes \mathbf{I}_{N_r} \right),$$

where ρ_{si} is the SI channel strength, \mathbf{H}_0 is a deterministic matrix of all-1 elements, and K_R is the Rician coefficient. The spatial covariance matrix of the estimated error is assumed to be the identity matrix. The overall system performance is averaged over 100 channel realizations. For numerical analysis, the default parameter values are chosen as in Table I.

$ \mathbb{K} = K$	4
$N = N_s = M_r = N_r = M_d$	2
$\rho = \rho_{sr} = \rho_{rd}$	-20 dB
$\rho_{sd}, \rho_{si}, K_R$	-30 dB, 0 dB, 1
$\sigma_n^2 = \sigma_{r,k}^2 = \sigma_{d,k}^2$	-30 dB
$P_{\max} = P_s = P_r$	0 dB
$P_{szero} = P_{zero} = P_{FD}$	-20 dB
$d = d_s = d_r$	2
$\kappa = \beta, \Theta_{tx,s} = \Theta_{tx,r} = \Theta_{rx,r} = \Theta_{rx,d} = \kappa \mathbf{I}_N$	-40 dB

TABLE I. DEFAULT SETUP

Comparison Benchmarks

For comparison using numerical simulations, the following benchmarks are considered:

- **JC**: It represents the proposed algorithms for joint-carrier (JC) design introduced in Subsection III-A1, with consideration of the impact of imperfect CSI as well as the hardware distortions.
- **PC**: It represents the proposed algorithms for per-carrier (PC) design introduced in Section III-A, with consideration of the impact of imperfect CSI as well as the hardware distortions.
- **LD** (less-distortion): It indicates the algorithms that do not consider the impact of hardware distortions at the source and the destination in the design, i.e., only hardware inaccuracy at the relay is considered since hardware impairments are more significant for FD nodes.
- **ND** (non-distortion) [32], [35]: It indicates the algorithms that do not consider the impact of hardware distortions in the design ($\kappa = \beta = 0$), i.e., a perfect hardware inaccuracy is assumed even though the system suffers from hardware distortions. It only considers the impact of imperfect CSI similar to [32], [35].
- **Wo-CSI** (without-CSI) [31]: It indicates the scenario where the system is able to attain a perfect CSI similar to [31]. However, here the impact of hardware distortions is taken into account.
- **HD** [50]: It indicates the scenarios when an HD MIMO relay is employed similar to [50]. We consider the HD relay utilizes TDD, hence SI is not present. Here, the

hardware distortions and channel estimation error are taken into consideration.

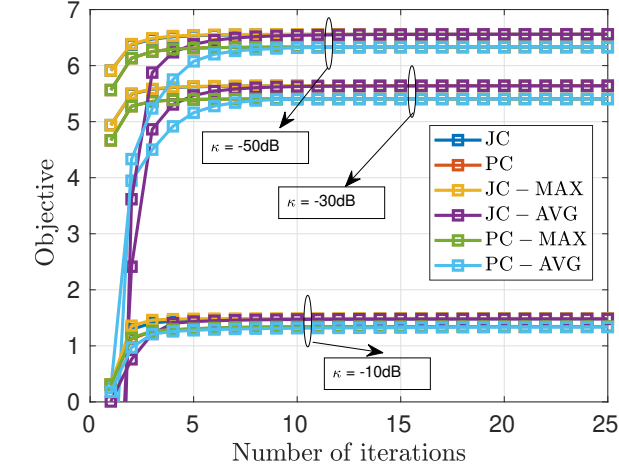
Visualization

In Fig. 1(a), the average convergence behaviour of our proposed solution with multiple initial points (random initializations) is plotted for different values of hardware inaccuracy κ dB. Here, we have observed that right singular matrix (RSM) initialization proposed in [47, Appendix A] shows a better convergence behavior compared to a random initialization, i.e., a slower convergence. It is observed that the algorithm converges within 10-25 iterations while utilizing the RSM initialization. As expected, it can be seen that the objective has a higher value for smaller hardware inaccuracy. However during numerical simulations, we have observed a optimality gap for higher hardware inaccuracies. This is expected, as larger κ leads to a more complex problem structure.

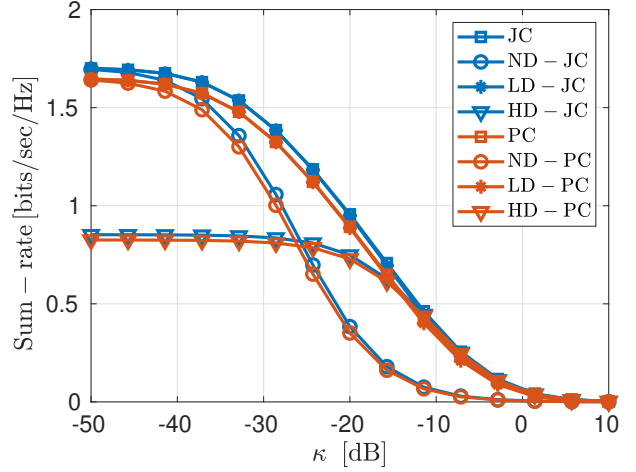
In Fig. 1(b), the performance of the proposed design (JC and PC), in terms of system sum-rate, is evaluated for different values of transceiver accuracy. As we can observe, the sum-rate decreases as the transceiver inaccuracy increases, i.e., the higher the κ , the smaller the sum-rate. It is clear that the proposed design JC outperforms all the other benchmarks. However, for small values of the transceiver inaccuracies, the ND algorithms (ND-JC and ND-PC) performance similar the proposed algorithms (JC and PC), respectively. As κ increases, the performance of ND algorithms degrades compared to the corresponding proposed algorithms. For higher values of κ , the HD algorithms performs better than the ND algorithms due to presence of strong SI, which implies that the consideration of a hardware-distortion aware design is significant for FD systems. It is also interesting to observe that the LD design performs similar to the JC design except for the higher values of κ , which is very unusual in the practical case.

In Fig. 1(c), the impact of the receiver noise in the system performance in terms sum-rate is depicted. As expected, it can be observed that the sum-rate of the system decreases as the receiver noise increases. The proposed algorithm (JC) shows better performance compared to all other benchmarks. It is interesting to observe that for lower values of receiver noise, the performance of the ND algorithms degrades compared to the proposed algorithms for both JC and PC design. This is due to the fact that, for lower values of receiver noise, the hardware distortions become dominant. This shows the importance of considering a hardware-distortion aware design, especially in high signal to noise ratio (SNR) scenario.

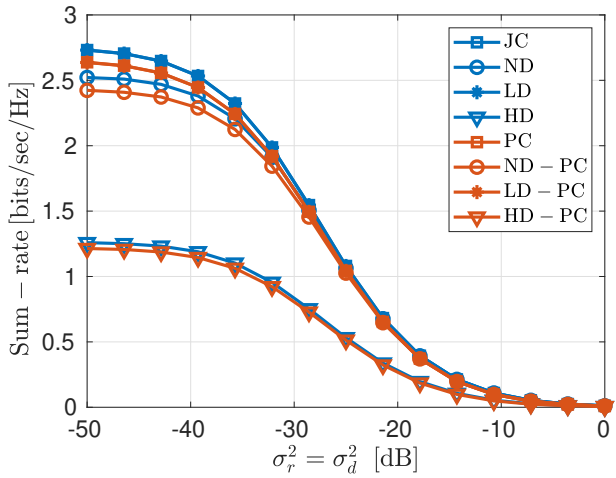
In Fig. 1(d), the performance of all the algorithms in terms of sum-rate is evaluated with respect to the channel estimation error. It can be clearly observed that as the channel estimation error increases the sum-rate of the system decreases. For higher values of channel estimation error, the performance of the Wo-CSI design becomes worst compared to the JC and ND designs, which shows the relevance of consideration of channel estimation error in the design. Another interesting observation, as in case of receiver noise, is that the performance of the ND-JC algorithm becomes worst compared to the proposed JC algorithm. This is because, for lower values of channel



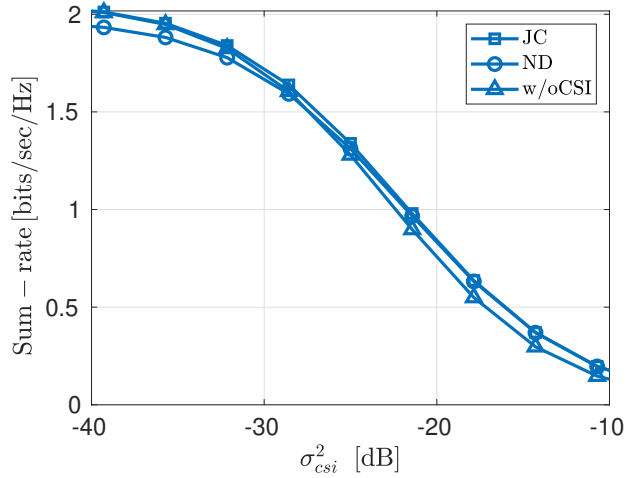
(a) Average Convergence Behaviour of JC and PC Algorithms



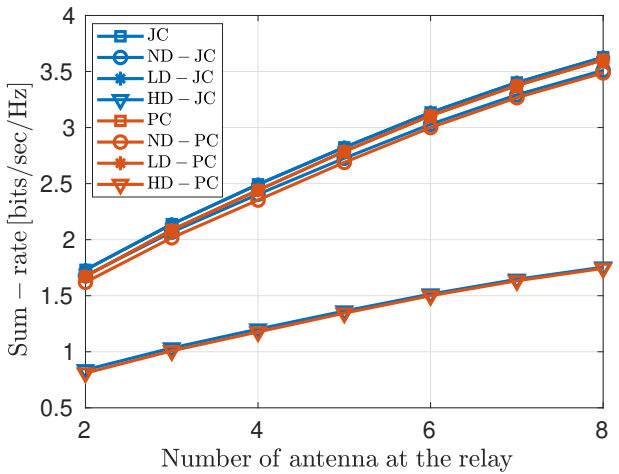
(b) Sum-rate vs. Hardware Inaccuracy



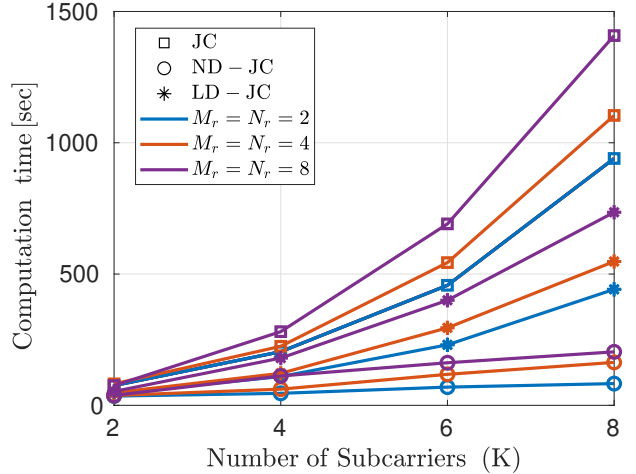
(c) Sum-rate vs. Receiver Noise



(d) Sum-rate vs. Channel Estimation Error

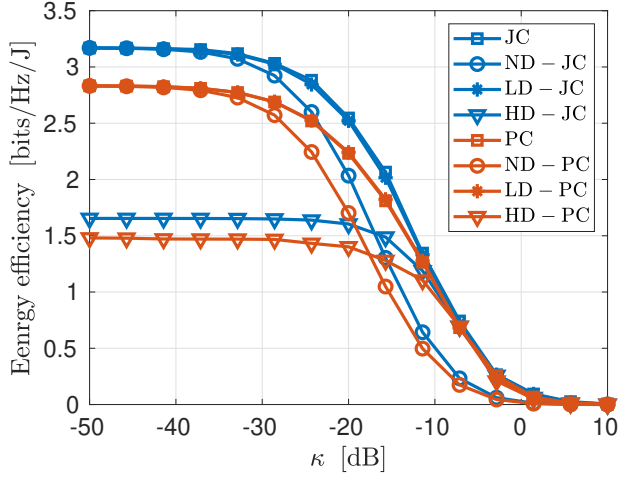


(e) Sum-rate vs. Number of Antennas at the Relay

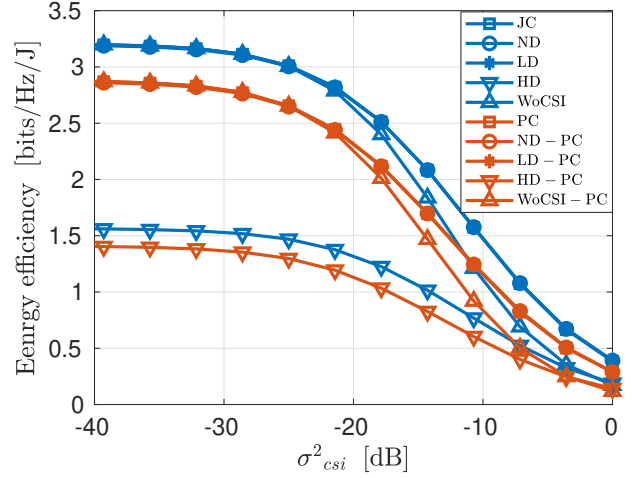


(f) Computation time vs. Number of Subcarriers

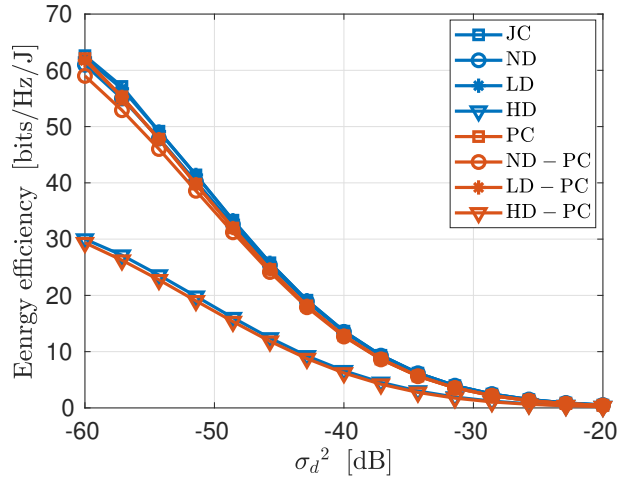
Fig. 1. Sum-rate vs. different system parameters



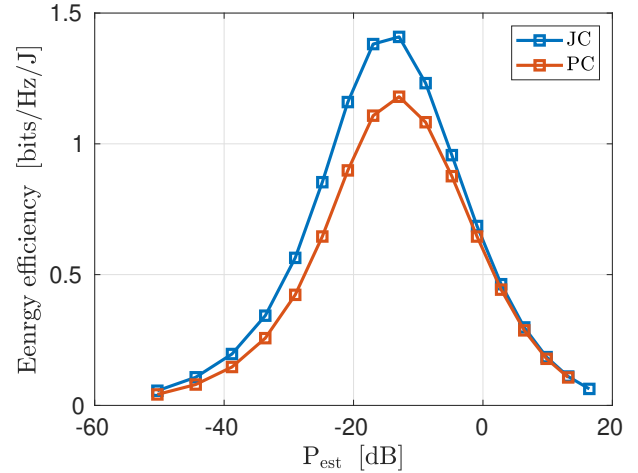
(a) Energy Efficiency vs. Hardware Inaccuracy.



(b) Energy Efficiency vs. Channel Estimation Error



(c) Energy Efficiency vs. Receiver Noise



(d) Energy Efficiency vs. Power Consumed for Channel Estimation

Fig. 2. Energy Efficiency vs. different system parameters

estimation error, the hardware distortion becomes dominant resulting in performance degradation of ND-JC algorithm.

In Fig. 1(e), the total sum-rate of the system is plotted against the number of antennas at the relay. As expected, the sum-rate generally increases as the number of antennas at the relay increases. An interesting observation is that as the number of antennas at the relay increases, the performance of ND algorithm degrades compared to the JC and PC algorithms. This implies that as the number of antennas increases, hardware-distortion aware design becomes more relevant.

Fig. 2(a) shows the impact of the transceiver inaccuracy on the energy efficiency of the system. We can observe a similar trend as in the case of the sum-rate. The energy efficiency of the system decreases as the transceiver inaccuracy (κ) increases. The performance of ND algorithms degrades compared to the corresponding proposed algorithms as the transceiver inaccuracies (κ) increases. Due to the absence

of SI, the HD systems becomes more energy efficient FD systems that does not consider hardware distortions for higher transceiver inaccuracies scenario. This can be clearly observed as the HD algorithms outperforms its ND counterpart for higher values of κ , which implies the importance of considering a hardware-distortion aware design. It is also observed that the ND design becomes less efficient compared to the JC design, as the value of (κ) increases.

Fig. 2(b) and 2(c) depicts the system performance in terms of energy efficiency with respect to different values of receiver noise and channel estimation error, respectively. As expected, it can be noticed that as the receiver noise or channel estimation error increases the energy efficiency of the system decreases. It can also be observed that the proposed algorithm outperforms their respective ND and HD benchmarks. In Fig. 2(b), it can be noticed that the energy efficiency of system with Wo-CSI design performs worst compared to the JC and ND design,

particularly for higher values of channel estimation error. This shows the significance of considering the channel estimation error in energy efficient system design. Furthermore in Fig. 2(c), we can observe that for lower values of receiver noise, the proposed algorithms outperforms their respective ND counterpart. This is because, the hardware distortions become more dominant when the receiver noise becomes less, which in turn degrades the performance of the ND algorithm. This shows the significance of hardware-distortion aware design to improve energy efficiency of FD systems, especially in high SNR scenario.

Fig. 2(d) shows the impact of power consumed for channel estimation on the energy efficiency of the system. Initially, the energy efficiency of the system increases as the power consumed for channel estimation increases. However after a certain point, the energy efficiency starts to degrade. This is because the energy required for the transmission becomes less as more power is allocated to the channel estimation. Hence, it is better to restrict the power consumption for channel estimation with some budget constraint to gain better energy efficiency.

Computational Complexity

In Table. II, the computational complexity of the algorithms in terms of the required computational time (CT) is depicted for different values of transceiver accuracy⁶. It can be seen that the JC design requires a high CT compared to other algorithms. This is due to the consideration of distortion of all the nodes as well as joint sub-carrier optimization. It is interesting to observe that LD design performs similar to the JC design with less CT. It also outperforms the PC design even though both designs require almost similar CT. Hence for complex systems, one can use LD design without significant degradation.

κ dB	JC	PC	LD	LD-PC	ND
-40	80.32	46.41	53.45	30.59	27.14
-20	63.18	46.15	53.45	30.59	27.18
-5	69.23	50.15	43.93	33.60	27.18

TABLE II. COMPARISON OF COMPUTATIONAL COMPLEXITY IN TERMS OF CT (SECS)

Fig. 1(f) illustrates the computational complexity of the JC algorithms in terms of the required computational time (CT) with respect to the number of sub-carriers K for different number of relay antennas. For this numerical simulation, we consider the value of transceiver inaccuracies (κ) to be -50 dB. As expected, it can be observed that the computational time increases as the number of sub-carriers or number of relay antennas ($M_r = N_r$) increases. As the number of sub-carriers increases, the algorithm complexity increases drastically compared to ND algorithm due to ICL introduced by non-linear hardware distortions. Another interesting observation is that the LD algorithm, which attains similar performance to proposed algorithm, has less computational complexity compared to JC algorithm.

⁶The reported CT is obtained using an Intel Core i7-4790S processor with a clock rate of 3.2 GHz and 16 GB RAM. We use MATLAB 2016b on a 64-bit operating system.

VI. CONCLUSION

MC FD systems are usually limited by the residual SI, which spreads over multiple subcarriers due to the non-linear hardware distortion. In this work, we have proposed linear transceiver design strategies for an FD MC MIMO DF relaying system, considering maximization of energy efficiency as well as the system sum-rate, while taking into account the impact of hardware impairments. From the numerical simulations, it is observed that a significant gain can be obtained via the application of the proposed distortion-aware designs, when transceiver inaccuracy increases, and ICL becomes a dominant factor. This indicates that the consideration of hardware distortion is essential for an FD MIMO MC relay system. Furthermore, it is observed that the JC approach performs better compared to the PC approach and the HD benchmarks. It can also be noticed that the LD approach, which is computationally less complex, performs almost similar to the proposed optimal design, and hence can be viewed as a viable alternative for more complex scenarios, e.g., a multi-user or large array setup, without a significant performance degradation.

As a future research step, we would like to address the application of ultra reliable low latency communications (URLLC) in mobile communications by consider low-density parity-check (LDPC) codes [51], [52] which are of great significance to improve the error performance of both HD and FD MIMO systems.

APPENDIX A

PROOF OF LEMMA II.1

The time domain statistical independence $e_{t,l}(t) \perp v_l(t)$ and $e_{t,l}(t) \perp e_{t,l'}(t)$, and the linear nature of the transformation (13) are also applicable to the statistical independence properties at the transformed unitary domain. Similarly, the Gaussian and zero-mean properties for $e_{t,l}^k$ becomes a linearly weighted sum of the zero-mean Gaussian values $e_{t,l}(mT_s)$. The variance of $e_{t,l}^k$ can hence be obtained as

$$\begin{aligned}
 \mathbb{E} \left\{ |e_{t,l}^k|^2 \right\} &= \mathbb{E} \left\{ \left(\sum_{m=0}^{N-1} e_{t,l}(mT_s) q_{k,m}^* \right) \times \left(\sum_{n=0}^{N-1} e_{t,l}^*(nT_s) q_{k,n} \right) \right\} \\
 &= \sum_{m=0}^{N-1} \sum_{n=0}^{N-1} \mathbb{E} \left\{ e_{t,l}(mT_s) e_{t,l}^*(nT_s) \right\} q_{k,m}^* q_{k,n} \\
 &= \sum_{m=0}^{N-1} \mathbb{E} \left\{ e_{t,l}(mT_s) e_{t,l}^*(mT_s) \right\} q_{k,m} q_{k,m}^* \quad (e_{t,l}(t) \perp e_{t,l}(t')) \\
 &= \kappa_l \mathbb{E} \left\{ |v_l(t)|^2 \right\} \quad (\text{from (12) and } \sum_{m=0}^{N-1} q_{k,m} q_{k,m}^* = 1) \\
 &= \frac{\kappa_l}{K} \sum_{m=1}^K \mathbb{E} \left\{ |v_l^m|^2 \right\} \quad (\text{Parseval's Theorem on energy conservation}).
 \end{aligned} \tag{48}$$

Similarly, the proof to the receiver characterization can be obtained.

REFERENCES

- [1] V. Radhakrishnan, O. Taghizadeh, and R. Mathar, "Linear Transceiver Design for Multi-Carrier Full-Duplex MIMO Decode and Forward

- Relaying,” in *WSA 2018; 22nd International ITG Workshop on Smart Antennas*, March 2018, pp. 1–6.
- [2] M. Shafi, A. F. Molisch, P. J. Smith, T. Haustein, P. Zhu, P. De Silva, F. Tufvesson, A. Benjebbour, and G. Wunder, “5g: A tutorial overview of standards, trials, challenges, deployment, and practice,” *IEEE journal on selected areas in communications*, vol. 35, no. 6, pp. 1201–1221, 2017.
 - [3] M. Duarte, C. Dick, and A. Sabharwal, “Experiment-Driven Characterization of Full-Duplex Wireless Systems,” *IEEE Transactions on Wireless Communications*, vol. 11, no. 12, pp. 4296–4307, December 2012.
 - [4] A. S. E. Everett and A. Sabharwal, “Passive Self-Interference Suppression for Full-Duplex Infrastructure Nodes,” *IEEE Transactions on Wireless Communications*, vol. 13, pp. 680–694, 2014.
 - [5] M. A. Khojastepour, K. Sundaresan, S. Rangarajan, X. Zhang, and S. Barghi, “The Case for Antenna Cancellation for Scalable Full-Duplex Wireless Communications,” in *Proceedings of the 10th ACM Workshop on Hot Topics in Networks*, ser. HotNets-X. New York, NY, USA: Association for Computing Machinery, 2011. [Online]. Available: <https://doi.org/10.1145/2070562.2070579>
 - [6] T. Riihonen and R. Wichman, “Analog and digital self-interference cancellation in full-duplex MIMO-OFDM transceivers with limited resolution in A/D conversion,” in *2012 Conference Record of the Forty Sixth Asilomar Conference on Signals, Systems and Computers (ASILOMAR)*, Nov 2012, pp. 45–49.
 - [7] M. S. Sim, M. Chung, D. Kim, J. Chung, D. K. Kim, and C. Chae, “Nonlinear Self-Interference Cancellation for Full-Duplex Radios: From Link- and System-Level Performance Perspectives,” *CoRR*, vol. abs/1607.01912, 2016. [Online]. Available: <http://arxiv.org/abs/1607.01912>
 - [8] D. Bharadia and S. Katti, “Full Duplex MIMO Radios,” in *11th USENIX Symposium on Networked Systems Design and Implementation (NSDI 14)*. Seattle, WA: USENIX Association, 2014, pp. 359–372. [Online]. Available: <https://www.usenix.org/conference/nsdi14/technical-sessions/bharadia>
 - [9] T. Riihonen, S. Werner, and R. Wichman, “Mitigation of loopback self-interference in full-duplex mimo relays,” *IEEE Transactions on Signal Processing*, vol. 59, no. 12, pp. 5983–5993, Dec 2011.
 - [10] S. Hong, J. Brand, J. Choi, M. Jain, J. Mehlman, S. Katti, and P. Levis, “Applications of self-interference cancellation in 5G and beyond,” *IEEE Communications Magazine*, vol. 52, pp. 114–121, 2014.
 - [11] R. A. Pitaval, O. Tirkkonen, R. Wichman, K. Pajukoski, E. Lahetkangas, and E. Tiirola, “Full-duplex self-backhauling for small-cell 5G networks,” *IEEE Wireless Communications*, vol. 22, no. 5, pp. 83–89, October 2015.
 - [12] O. Taghizadeh, V. Radhakrishnan, A. C. Cirik, R. Mathar, and L. Lampe, “Hardware Impairments Aware Transceiver Design for Bidirectional Full-Duplex MIMO OFDM Systems,” *IEEE Transactions on Vehicular Technology*, vol. 67, no. 8, pp. 7450–7464, Aug 2018.
 - [13] B. P. Day, A. R. Margetts, D. W. Bliss, and P. Schniter, “Full-Duplex MIMO Relaying: Achievable Rates Under Limited Dynamic Range,” in *IEEE Journal on Selected Areas in Communications*, 2012.
 - [14] O. Taghizadeh, A. C. Cirik, R. Mathar, and L. Lampe, “Sum power minimization for tdd-enabled full-duplex bi-directional mimo systems under channel uncertainty,” in *European Wireless 2017; 23th European Wireless Conference*, 2017, pp. 1–6.
 - [15] J. Zhang, O. Taghizadeh, and M. Haardt, “Robust transmit beamforming design for full-duplex point-to-point mimo systems,” in *ISWCS 2013; The Tenth International Symposium on Wireless Communication Systems*, 2013, pp. 1–5.
 - [16] T. Yang, O. Taghizadeh, and R. Mathar, “Sum secrecy rate maximization for multi-carrier mimome systems with full-duplex jamming,” *Physical Communication*, vol. 35, p. 100730, 2019.
 - [17] O. Taghizadeh, P. Neuhaus, R. Mathar, and G. Fettweis, “Secrecy energy efficiency of mimome wiretap channels with full-duplex jamming,” *IEEE Transactions on Communications*, vol. 67, no. 8, pp. 5588–5603, 2019.
 - [18] O. Taghizadeh, P. Sirvi, S. Narasimha, J. A. L. Calvo, and R. Mathar, “Environment-aware minimum-cost wireless backhaul network planning with full-duplex links,” *IEEE Systems Journal*, vol. 13, no. 3, pp. 2582–2593, 2019.
 - [19] A. C. Cirik, S. Biswas, O. Taghizadeh, and T. Ratnarajah, “Robust transceiver design in full-duplex mimo cognitive radios,” *IEEE Transactions on Vehicular Technology*, vol. 67, no. 2, pp. 1313–1330, 2018.
 - [20] S. Biswas, K. Singh, O. Taghizadeh, and T. Ratnarajah, “Coexistence of mimo radar and fd mimo cellular systems with qos considerations,” *IEEE Transactions on Wireless Communications*, vol. 17, no. 11, pp. 7281–7294, 2018.
 - [21] A. Sabharwal, P. Schniter, D. Guo, D. W. Bliss, S. Rangarajan, and R. Wichman, “In-Band Full-Duplex Wireless: Challenges and Opportunities,” *IEEE Journal on Selected Areas in Communications*, vol. 32, no. 9, pp. 1637–1652, Sept 2014.
 - [22] O. Taghizadeh, M. Rothe, A. C. Cirik, and R. Mathar, “Distortion-loop analysis for full-duplex amplify-and-forward relaying in cooperative multicast scenarios,” in *2015 9th International Conference on Signal Processing and Communication Systems (ICSPCS)*, Dec 2015, pp. 1–9.
 - [23] O. Taghizadeh, A. C. Cirik, and R. Mathar, “Hardware impairments aware transceiver design for full-duplex amplify-and-forward MIMO relaying,” *IEEE Transactions on Wireless Communications*, vol. 17, no. 3, pp. 1644–1659, Mar. 2018.
 - [24] M. Heino, D. Korpi, T. Huusari, E. Antonio-Rodriguez, S. Venkatasubramanian, T. Riihonen, L. Anttila, C. Icheln, K. Haneda, R. Wichman, and M. Valkama, “Recent advances in antenna design and interference cancellation algorithms for in-band full duplex relays,” *IEEE Communications Magazine*, vol. 53, no. 5, pp. 91–101, May 2015.
 - [25] H. Shen, C. Liu, W. Xu, and C. Zhao, “Optimized Full-Duplex MIMO DF Relaying With Limited Dynamic Range,” *IEEE Access*, vol. 5, pp. 20726–20735, 2017.
 - [26] O. Taghizadeh and R. Mathar, “Full-duplex decode-and-forward relaying with limited self-interference cancellation,” in *WSA 2014; 18th International ITG Workshop on Smart Antennas*, 2014, pp. 1–7.
 - [27] O. Taghizadeh and R. Mathar, “Robust multi-user decode-and-forward relaying with full-duplex operation,” in *The Eleventh International Symposium on Wireless Communication Systems (ISWYS 2014)*, Barcelona, Spain, Sep. 2014, pp. 1–7.
 - [28] H. Liu, K. J. Kim, K. S. Kwak, and H. V. Poor, “Power Splitting-Based SWIPT With Decode-and-Forward Full-Duplex Relaying,” *IEEE Transactions on Wireless Communications*, vol. 15, no. 11, pp. 7561–7577, Nov 2016.
 - [29] J. Ko, M. Jung, and H. Jin, “Outage analysis of full-duplex DF relaying with limited dynamic range of ADC,” in *2016 IEEE 27th Annual International Symposium on Personal, Indoor, and Mobile Radio Communications (PIMRC)*, Sept 2016, pp. 1–6.
 - [30] C. Li, Z. Chen, Y. Wang, Y. Yao, and B. Xia, “Outage Analysis of the Full-Duplex Decode-and-Forward Two-Way Relay System,” *IEEE Transactions on Vehicular Technology*, vol. 66, no. 5, pp. 4073–4086, May 2017.
 - [31] B. Yu, L. Yang, X. Cheng, and R. Cao, “Power and location optimization for full-duplex decode-and-forward relaying,” *IEEE Transactions on Communications*, vol. 63, no. 12, pp. 4743–4753, 2015.
 - [32] R. Patidar, S. Duwasha, and R. Dubey, “Decode-And-Forward Full Duplex relaying in MIMO-OFDMA Systems,” *International journal of innovative research in electrical, electronics, instrumentation and control engineering*, vol. 1, no. 6, September 2013.
 - [33] L. Chen, W. Meng, and Y. Hua, “Optimal power allocation for a full-duplex multicarrier decode-forward relay system with or without direct link,” *Signal Processing*, vol. 137, pp. 177–191, 2017.
 - [34] S. Wang, W. Yang, and W. Xu, “Outage analysis of OFDM Full Duplex relaying systems,” in *2015 International Conference on Wireless Communications Signal Processing (WCSP)*, Oct 2015, pp. 1–4.

- [35] D. W. K. Ng, E. S. Lo, and R. Schober, "Dynamic resource allocation in mimo-ofdma systems with full-duplex and hybrid relaying," *IEEE Transactions on Communications*, vol. 60, no. 5, pp. 1291–1304, May 2012.
- [36] M. Mokhtar, N. Al-Dhahir, and R. Hamila, "Ofdm full-duplex df relaying under i/q imbalance and loopback self-interference," *IEEE Transactions on Vehicular Technology*, vol. 65, no. 8, pp. 6737–6741, 2016.
- [37] U. Tefek and T. J. Lim, "Full-duplex simo relaying for machine-type communications in cellular networks," in *2017 IEEE 86th Vehicular Technology Conference (VTC-Fall)*, 2017, pp. 1–6.
- [38] R. Pabst, B. H. Walke, D. C. Schultz, P. Herhold, H. Yanikomeroglu, S. Mukherjee, H. Viswanathan, M. Lott, W. Zirwas, M. Dohler *et al.*, "Relay-based deployment concepts for wireless and mobile broadband radio," *IEEE Communications magazine*, vol. 42, no. 9, pp. 80–89, 2004.
- [39] B. P. Day, D. W. Bliss, A. R. Margetts, and P. Schniter, "Full-duplex bidirectional MIMO: Achievable rates under limited dynamic range," in *2011 Conference Record of the Forty Fifth Asilomar Conference on Signals, Systems and Computers (ASILOMAR)*, Nov 2011, pp. 1386–1390.
- [40] O. Taghizadeh, A. C. Cirik, and R. Mathar, "Hardware Impairments Aware Transceiver Design for Full-Duplex Amplify-and-Forward MIMO Relaying," *IEEE Transactions on Wireless Communications*, vol. 17, no. 3, pp. 1644–1659, Mar 2018.
- [41] D. Xu, P. Ren, and J. A. Ritcey, "Independence-checking coding for ofdm channel training authentication: Protocol design, security, stability, and tradeoff analysis," *IEEE Transactions on Information Forensics and Security*, vol. 14, no. 2, pp. 387–402, 2019.
- [42] W. Namgoong, "Modeling and analysis of nonlinearities and mismatches in ac-coupled direct-conversion receiver," *IEEE Transactions on Wireless Communications*, vol. 4, no. 1, pp. 163–173, Jan 2005.
- [43] G. Santella and F. Mazzenga, "A hybrid analytical-simulation procedure for performance evaluation in m-qam-ofdm schemes in presence of nonlinear distortions," *IEEE Transactions on Vehicular Technology*, vol. 47, no. 1, pp. 142–151, Feb 1998.
- [44] H. Suzuki, T. V. A. Tran, I. B. Collings, G. Daniels, and M. Hedley, "Transmitter noise effect on the performance of a mimo-ofdm hardware implementation achieving improved coverage," *IEEE Journal on Selected Areas in Communications*, vol. 26, no. 6, pp. 867–876, August 2008.
- [45] S. S. Christensen, R. Agarwal, E. D. Carvalho, and J. M. Cioffi, "Weighted sum-rate maximization using weighted MMSE for MIMO-BC beamforming design," *IEEE Transactions on Wireless Communications*, vol. 7, no. 12, pp. 4792–4799, December 2008.
- [46] J. Jose, N. Prasad, M. Khojastepour, and S. Rangarajan, "On robust weighted-sum rate maximization in mimo interference networks," in *2011 IEEE International Conference on Communications (ICC)*, June 2011, pp. 1–6.
- [47] H. Shen, B. Li, M. Tao, and X. Wang, "MSE-Based Transceiver Designs for the MIMO Interference Channel," *IEEE Transactions on Wireless Communications*, vol. 9, no. 11, pp. 3480–3489, November 2010.
- [48] W. Dinkelbach, "On nonlinear fractional programming," *Management Science*, vol. 13, no. 7, pp. 492–498, 1967.
- [49] A. Ben-Tal and A. Nemirovski, "Lectures on modern convex optimization: analysis, algorithms, and engineering applications," *Siam*, 2001.
- [50] T. Li, H. Yu, and S. Liu, "Adaptive power allocation for decode-and-forward mimo-ofdm relay system," in *2009 5th International Conference on Wireless Communications, Networking and Mobile Computing*, 2009, pp. 1–4.
- [51] Y. Fang, P. Chen, G. Cai, F. C. M. Lau, S. C. Liew, and G. Han, "Outage-limit-approaching channel coding for future wireless communications: Root-protograph low-density parity-check codes," *IEEE Vehicular Technology Magazine*, vol. 14, no. 2, pp. 85–93, 2019.
- [52] P. Chen, Z. Xie, Y. Fang, Z. Chen, S. Mumtaz, and J. J. P. C. Rodrigues, "Physical-layer network coding: An efficient technique for wireless communications," *IEEE Network*, vol. 34, no. 2, pp. 270–276, 2020.